Cooperativity Between Al–sites Promotes Hydrogen-Transfer and Carbon–Carbon Bond Formation Upon Dimethylether Activation on Alumina

Aleix Comas-Vives,[†] Maxence Valla,[†] Christophe Copéret[†,*] and Philippe Sautet[‡,*]

[†] ETH Zürich, Department of Chemistry and Applied Biosciences, Vladimir Prelog Weg 2, CH-8093 Zürich, Switzerland.

[‡] Université de Lyon, CNRS, Institut de Chimie de Lyon, École Normale Supérieure de Lyon, 46 allée d'Italie, F-69364 Lyon Cedex 07, France.

1. Additional Experimental Data
2. Description of the Model of γ-Al_2O_3 and Computational Details.
3. Additional Evaluated Reaction Mechanisms

1. Additional Experimental Data

1.1 Experimental details

The alumina samples were a boehmite-derived pure γ-Al_2O_3 with a specific surface area of 230 $m^2.g^{-1}$ provided by Sasol (**SBa-200**) and a pyrogenic Al_2O_3 with a surface area of *approx.* 130 $m^2.g^{-1}$ (Evonik/Degussa **Alu C**), composed of γ and δ-phase.

A pellet of Al_2O_3 (AluC or SBa 200) was pressed and loaded in a reactor equipped with CaF_2 windows on the head allowing the measure of *in situ* infrared spectra. The pellet was calcined at 500°C under static air for 12 h and treated under vacuum for 16 h at 700°C. Dry dimethyl ether, stored over 3A molecular sieves, was added to the reactor (40 mBar, 4.6 molecules per nm^2) contained alumina, and the reaction mixture was treated at different temperatures (25°C, 200°C and 300°C during 12 hours). At each step, IR spectra were recorded, and the gas phase was analyzed. For the removal of the surface hydrocarbons, the pellet was evacuated at 100°C under high vacuum, the gas phase was condensed in a liquid nitrogen trap. The gas phase was then concentrated and analyzed by GC (equipped with a HP-Plot Q column).

1.2 Additional Spectra and Experimental Data

Table S1. Desorbed compounds (molecules/nm^2) from Al_2O_3 (Sba 200, partially dehydroxylated at 700°C) after reaction with dimethyl ether at 300°C.

Hydrocarbon removed from the surface	Molecules per nm^2
Ethylene	$0.5x10^{-2}$
Propylene	$0.5x10^{-2}$
2-butene	$3.1x10^{-2}$
Pentene	$2.1x10^{-2}$
C6	Traces
C7	Traces

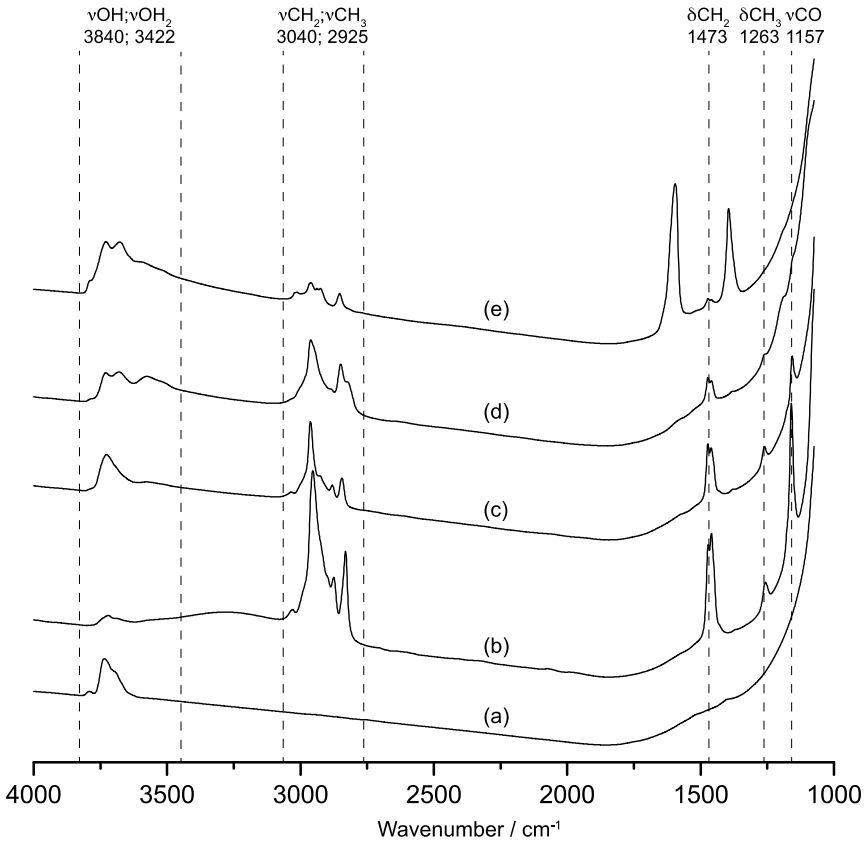

Figure S1. FT-IR Transmission spectra of Alu C Al_2O_3 (a) partially dehydroxylated at 700°C, (b) contacted with 40 mBar of dimethyl ether at room temperature, (c) after evacuation under high vacuum for 14 h, (d) after reaction with dimethyl ether at 200°C (e) after reaction with dimethyl ether at 300°C. All the spectra were recorded with the gas phase condensed at -190°C. The number of scans was 16.

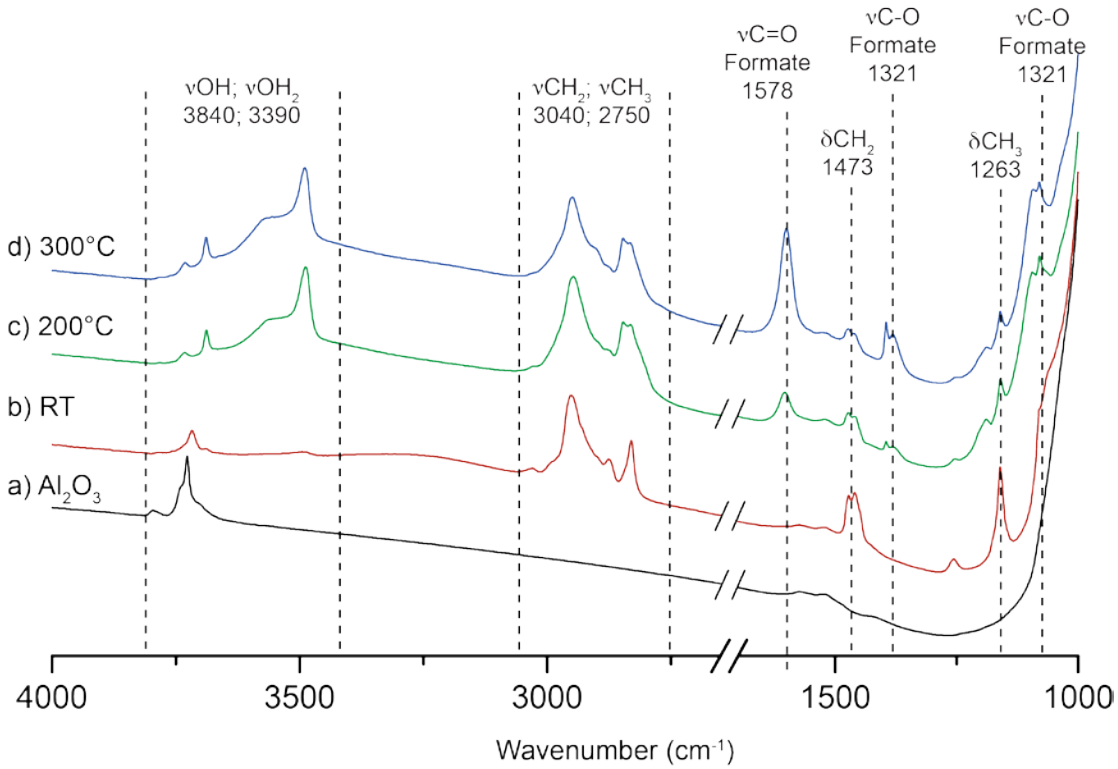

Figure S2.. FT-IR transmission spectra of (a) γ-alumina (Sba 200) Al_2O_3 partially dehydroxylated at 700°C, (b) after contacting with 40 mBar of dimethyl ether at room temperature, (c) after evacuation of the gas phase under high vacuum for 14 h (c), after reaction with dimethyl ether at 200°C (d) and after reaction with dimethyl ether at 300°C (e). All the spectra were recorded with the gas phase condensed at –190°C. The number of scans was 16.

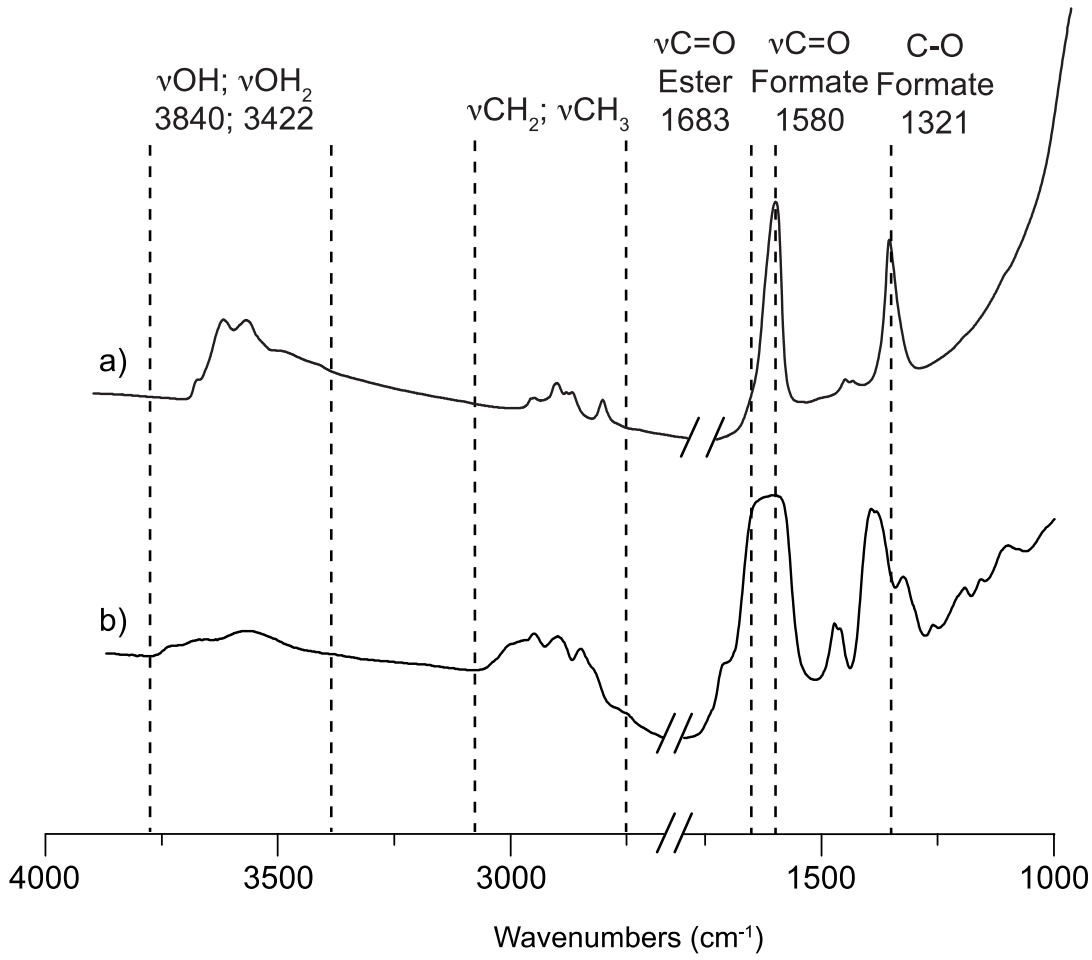

Figure S3. FT-IR transmission spectrum of a) DME contacted with Al_2O_3 at 300°C and b) methyl formate contacted with AluC (Evonik/Degussa)Al_2O_3 (700°C)

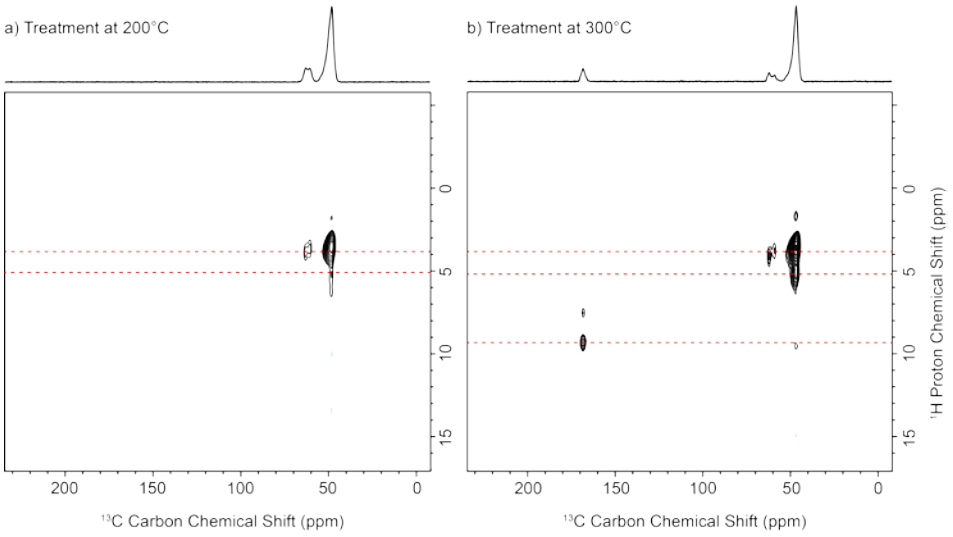

Figure S4. ^{1}H-^{13}C HETCOR, 400 MHz, 10 kHz, of AluC reacted with 2-^{13}C-$(CH_3)_2O$ at (a) 200°C and at (b) 300°C.

Figures S4a and S4b show similar features: the peaks at 62 and 64 ppm correlate with proton at 3.8 ppm, while the peak at 48 ppm correlates with protons at both 3.8 and 5.3 ppm. The signal at 3.8 ppm could be assigned to be proton attached to a methoxy group where the peak at 5.2 ppm could come from the OH from the alumina surface. Note that on the product treated at 300°C the 5.3 ppm proton have a stronger signal compare to the product treated at 200°C. The signal at 169 ppm correlates with a proton peak at 9.2 ppm, consistent with methyl formate species.

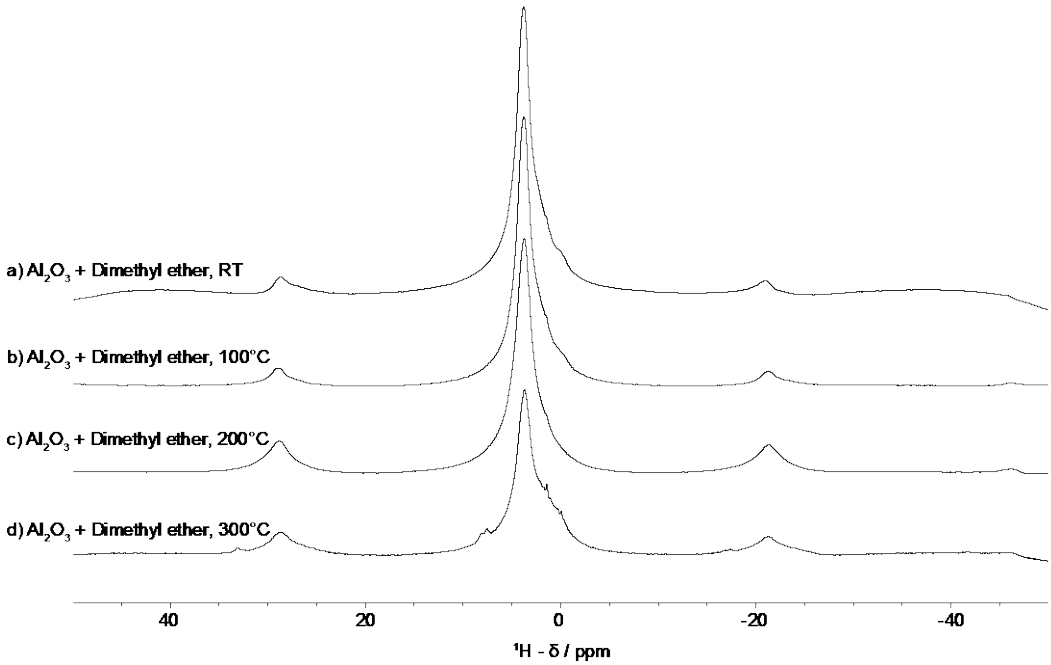

Figure S5. ^{1}H NMR, 400 MHz, 10 kHz, of Al_2O_3 reacted with 2-^{13}C-$(CH_3)_2O$ at (a) room temperature, number of scans: 32; (b) 100°C, number of scans: 32; (c) 200°C, number of scans: 32; and (d) 300°C, number of scans: 32.

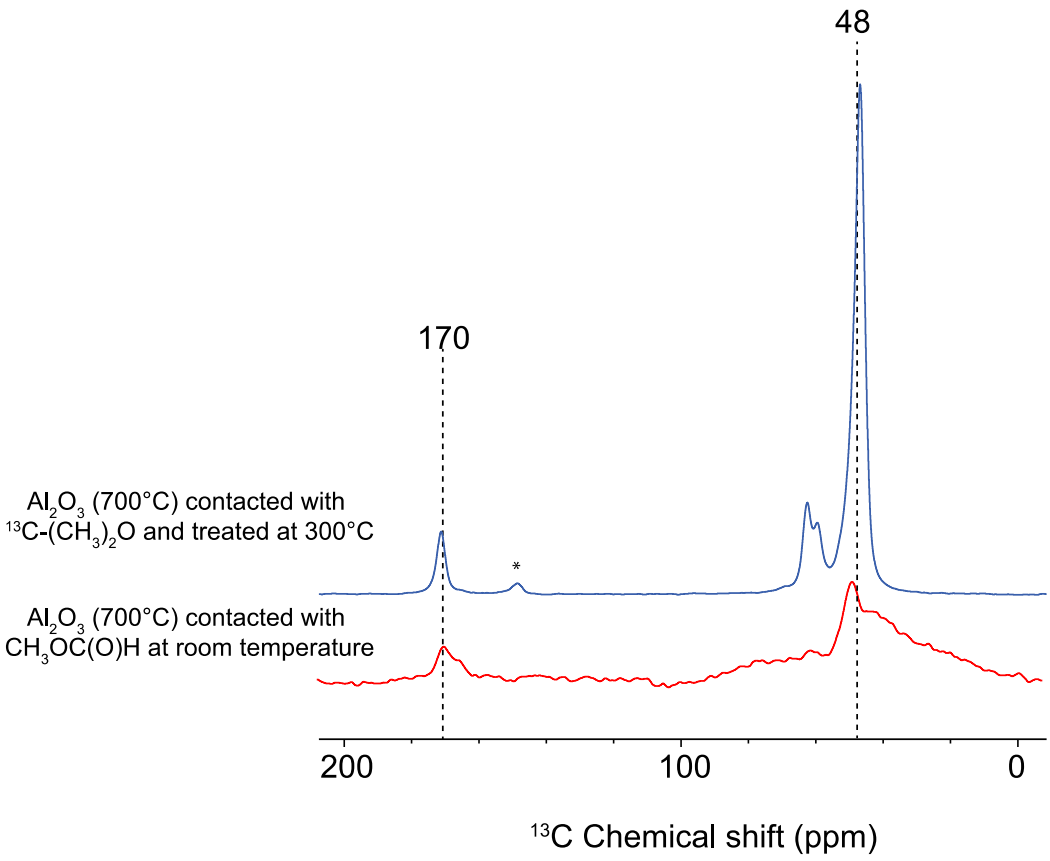

Figure S6. ^{1}H-^{13}C CPMAS, 400 MHz, 10 kHz, of AluC reacted with 2-^{13}C-$(CH_3)_2O$ at 300°C (blue, top spectrum) and AluC reacted with methyl formate at room temperature (red, bottom spectrum). Asterisk represents spinning side band.

2. Description of the Model of γ-Al_2O_3 and Computational Details

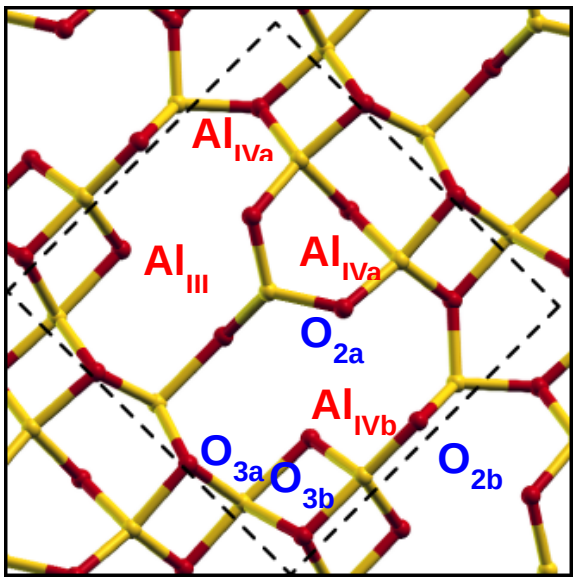

0

Figure S7. Model for the 110 termination of the γ-Al_2O_3 fully dehydroxylated (**s0** surface). A dashed line indicates the unit cell. Al: yellow, O: red balls.

For the description of Al_2O_3 we use a model with nonspinel sites occupied, based on the simulated dehydration of boehmite.[1] The γ-Al_2O_3 model has three type of Al centers: one tri-coordinated (Al_{III}) and two tetra-coordinated (Al_{IVa} and Al_{IVb}), whose Lewis acidity follows in decreasing order $Al_{(III)} > Al_{IVb} > Al_{IVa}$.

DFT calculations in periodic boundary conditions are carried out in the Perdew-Wang (PW91) implementation[2] of the generalized gradient approximation (GGA) for the correlation and exchange energy functional, using the VASP code (version 5.2).[3] The projected augmented wave (PAW)[4] method was adopted for describing electron-ion interactions. The climbing nudge elastic band method (CI-NEB)[5] was used to determine transition-states. The (110) surface of γ- (or δ-) Al_2O_3 is based on a previous established model,[1b] being described by a 8.07 x 8.40 Å unit cells and 8-layers (unit formula $Al_{32}O_{48}$). The inner-slab distance is *ca.* 24 Å. The Brilloun zone integration is performed with a 3 x 3 x 1 *k*-point grid generated by the Monkhorst-Pack algorithm. In order to reproduce the properties of extended surfaces, the bottom two-layers were kept fixed during the calculation at bulk coordinates, while the top layers were allowed to relax. For some calculations we took the dehydrated unit cell of γ-Al_2O_3 since the experimental OH density for the γ-Al_2O_3 surface pretreated at

700 °C under high vacuum during 12 h is equal to 0.7 OH/nm^2.[6] We included the effect of having one additional water on the unit cell for the finally proposed mechanism (corresponding to an OH coverage equal to 3.0 OH/nm^2).

3. Alternative Evaluated Reaction Mechanisms.

3.1 Alternative evaluated pathway involving the C-H activation of the DME molecule

Scheme S1. Calculated reaction pathway for the reaction of CH_3OCH_3 on γ-Al_2O_3 leading to the formation of $CH_3CH_2OCH_3$ as an intermediate and ethylene as a final product.

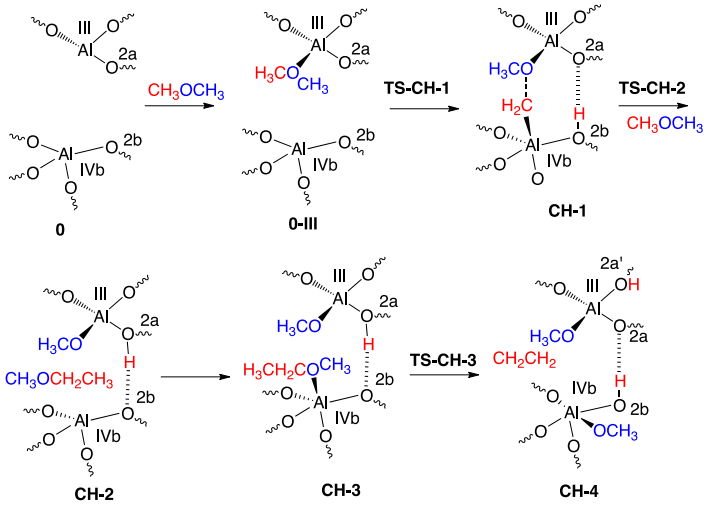

In view of the reactivity of methane and H_2 with Al_{III} sites, we examined the C-H bond activation of CH_3OCH_3 starting from **0-III** species This yields **CH-1** which is 105 kJ.mol^{-1} more stable than the separated reactants. During that process, the resulting CH_2 group coordinates to Al_{IVb} and the proton is transferred to the O_{2b} center in close vicinity with the O_{2a} atom, while OCH_3 stays coordinated to Al_{III}. This process is associated with an energy barrier of 144 kJ.mol^{-1} with respect to **0-III** species, a transition-state energy (or in other words an apparent energy barrier) of 12 kJ.mol^{-1} above separated reactants as depicted in Figure S7.

From **CH-1**, the C-H bond activation of second CH_3OCH_3 molecule on "Al–CH_2–OCH_3", a carbenoid species, which can in principle insert in the C-H bond and lead to the formation of a C-C bond. This step is strongly exoenergetic by 177 kJ.mol^{-1} with respect to **CH-1**, and it is associated with an energy barrier of 179 kJ.mol^{-1} (**TS-CH-**

2). This step yields $CH_3CH_2OCH_3$, which can further coordinate the adjacent Al_{IVb}, the most acidic Al center after Al_{III}. This step is exoenergetic by 73 kJ.mol^{-1} and corresponds to a reaction energy of –356 kJ.mol^{-1} with respects to the initial reactants (**CH-3** in Scheme S1). $CH_3CH_2OCH_3$ can further react with the alumina surface to yield ethylene with the transfer of OCH_3 to Al_{IVb} and a proton to an adjacent oxygen atom. This step has an energy barrier equal to 132 kJ.mol^{-1}. Overall, the rate-limiting step for the whole pathway for the ethylene formation via the formation of the $CH_3CH_2OCH_3$ intermediate is the C-H insertion, with an energy barrier of 179 kJ.mol^{-1}. Note that the resulting $CH_3CH_2OCH_3$ species could also react in an analogous way to dimethylether in order to form species with longer carbon-carbon bond chains. In **Figure S7**, it is shown the complete energy profile for this pathway. The apparent activation energy is equal to 73 kJ.mol^{-1}, whereas from the structure in which DME binds the AlIII center (**0-III**) to the highest point in the energy profile (**TS-CH-2**) the energetic difference equals 204 kJ.mol^{-1}.

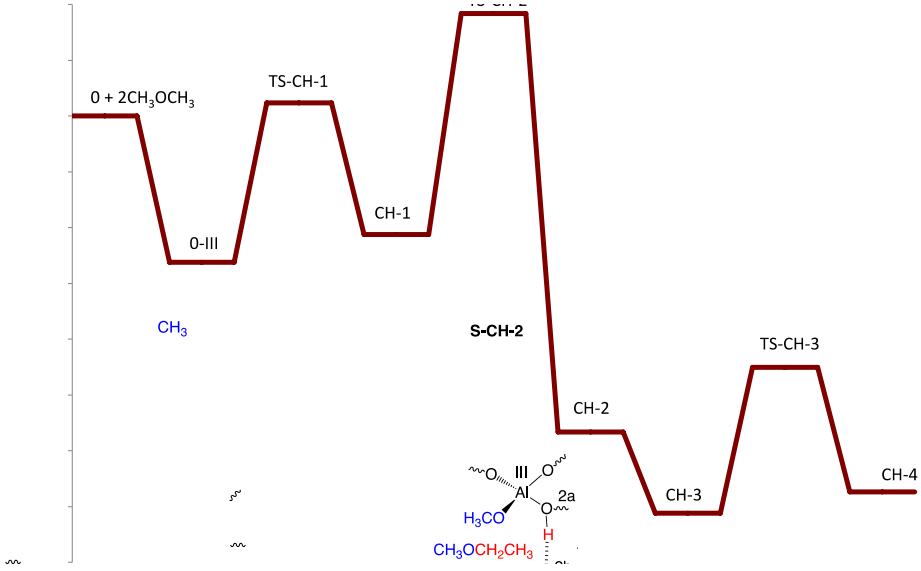

Figure S8: Energy profile (in kJ.mol^{-1}) for the formation of ethylene with the initial C-H activation of dimethylether.

3.2 Non-assisted C-O Activation Step

Scheme S2. Non-assisted C-O activation step of the DME molecule.

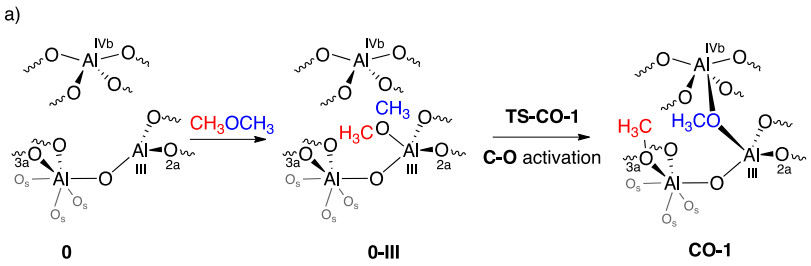

The non-assisted C-O activation step has a relative energy barrier equal to 179 kJ.mol^{-1}[1]. It was hence discarded as initial activation of the dimethylether molecule.

3.3 Comparison between analogous evaluated routes for the ethylene formation on surfaces with water on different initial surface sites (s1a, s1b and s1b2 surface)

The **s1b** and **s1b2** surface contain water on the Al_{IVb} center. In the former case (**s1b**) water is adsorbed in a dissociative way and the surface reconstructs as described previously.[6] The **s1b2** surface corresponds to a surface in which water coordinates to Al_{IVb} without initially reconstructing. The energy profiles for the ethylene formation from the **s1a**, **s1b** and **s1b2** surfaces are shown in **Figure S8**. For the **s1b** and **s1b2** surfaces the reaction steps are the same than the ones described on the main text for the **s1a** surface with the difference than in this case the dimethylether molecule initially coordinates to the Al_{III} center since for both surfaces this Al center is free. The **s1b2** surface reconstructs after the initial C-O activation step leading to the same structure than the product of the C-O activation on the **s1b** surface.

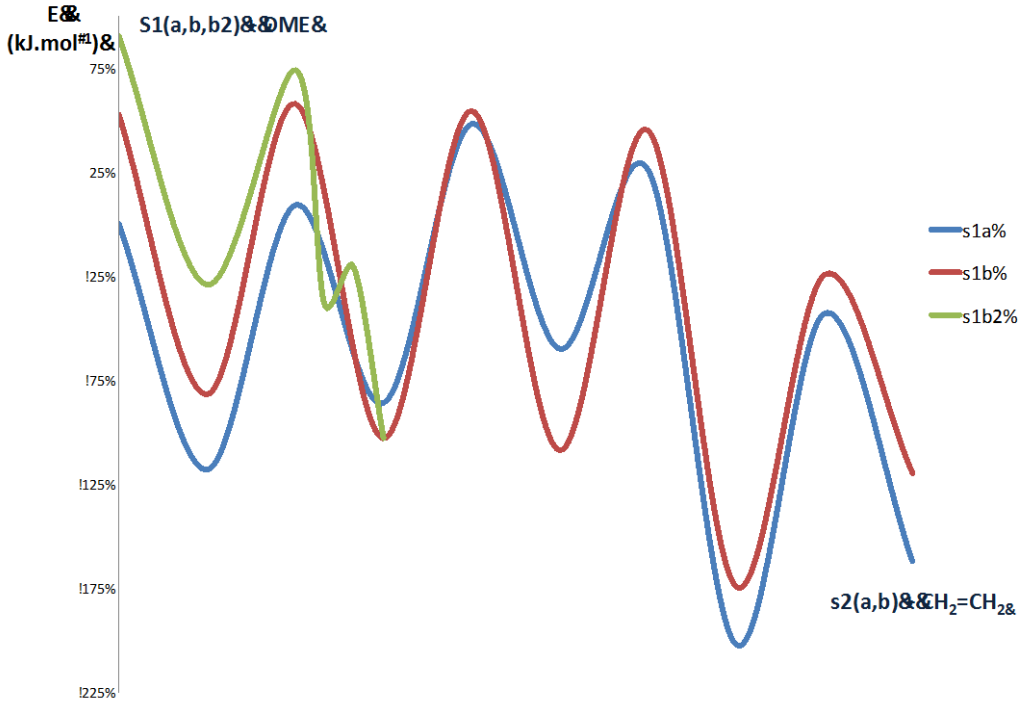

Figure S9. Comparison between the energy profiles corresponding to the ethylene formation for the **s1a**, **s1b** and **s1b2** surfaces. The energies (in kJ.mol^{-1}) are referred to the **s1a** surface and one dimethylether molecule.

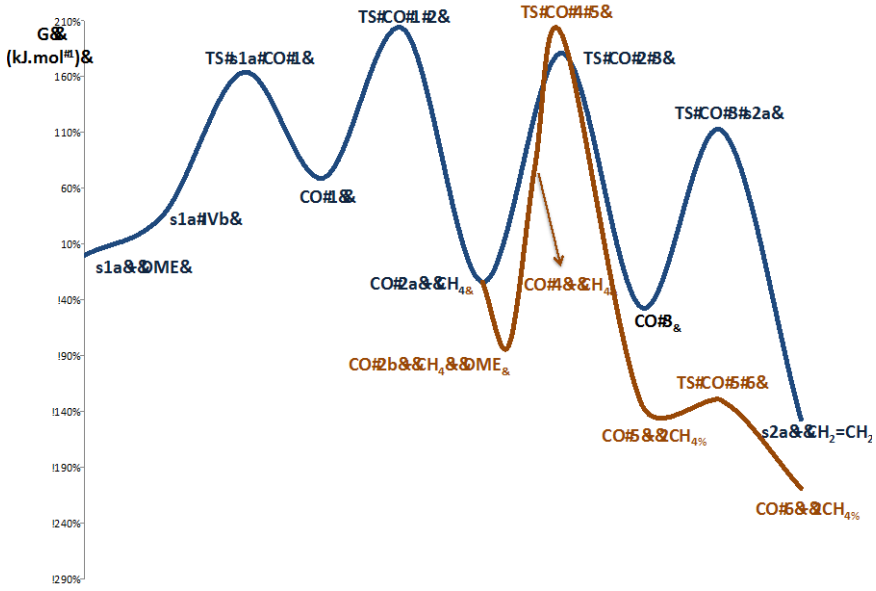

Figure S10. Gibbs free energy profiles (in kJ.mol^{-1}) on the **s1a** surface for the pathways of ethylene (in dark blue) and formate (in brown) formation, respectively.

References

1. (a) Krokidis, X.; Raybaud, P.; Gobichon, A. E.; Rebours, B.; Euzen, P.; Toulhoat, H., *J. Phys. Chem. B* **2001,** *105*, 5121-5130; (b) Digne, M.; Sautet, P.; Raybaud, P.; Euzen, P.; Toulhoat, H., *J. Catal.* **2004,** *226*, 54-68.
2. Perdew, J. P.; Chevary, J. A.; Vosko, S. H.; Jackson, K. A.; Pederson, M. R.; Singh, D. J.; Fiolhais, C., *Phys. Rev. B* **1992,** *46*, 6671.
3. (a) Kresse, G.; Furthmüller, J., *Comput. Mat. Sci.* **1996,** *6*, 15; (b) Kresse, G.; Furthmüller, J., *Phys. Rev. B* **1996,** *54*, 11169.
4. (a) Blöchl, P. E., *Phys. Rev. B* **1994,** *50*, 17953; (b) Kresse, G.; Joubert, D., *Phys. Rev. B* **1999,** *59*, 1758.
5. (a) Henkelman, G.; Uberuaga, B. P.; Jonsson, H., *J. Chem. Phys.* **2000,** *113*, 9901-9904; (b) Henkelman, G.; Jonsson, H., *J. Chem. Phys.* **2000,** *113*, 9978-9985.
6. Wischert, R.; Laurent, P.; Copéret, C.; Delbecq, F.; Sautet, P., *J. Am. Chem. Soc.* **2012,** *134*, 14430-14449.